

## Synthesis of Mesoporous Silica Particles and Capsules by Miniemulsion Technique

Renate Schiller,<sup>†</sup> Clemens K. Weiss,<sup>†</sup> Jasmin Geserick,<sup>‡</sup> Nicola Hüsing,<sup>‡</sup> and Katharina Landfester<sup>\*,†,§</sup>

<sup>†</sup>Max Planck Institute for Polymer Research, Ackermannweg 10, 55128 Mainz, Germany,

<sup>‡</sup>University of Ulm, Institute of Inorganic Chemistry I, Albert-Einstein-Allee 11, 89081 Ulm, Germany, and

<sup>§</sup>University of Ulm, Institute of Organic Chemistry III, Albert-Einstein-Allee 11, 89081 Ulm, Germany

Received June 29, 2009. Revised Manuscript Received September 23, 2009

Mesoporous silica particulate structures of different morphologies from particles to capsules have been prepared by combining the sol–gel process with the cooperative self-assembly in inverse miniemulsion. We report a novel synthetic approach at room temperature, with low surfactant concentrations (5 and 10 mol %, relative to the precursor), and a short synthesis time of only a few hours. As a precursor, glycol-modified silane (tetrakis(2-hydroxyethyl)orthosilicate, EGMS) is used, which shows the advantage of being highly water-soluble. The precursor (EGMS) and the structuring surfactant (cetyltrimethylammonium bromide, CTAB) were dissolved in hydrochloric acid and dispersed in a mixture of hydrocarbons (Isopar M) by ultrasonication. In this synthesis, two different surfactants were used simultaneously. One surfactant (CTAB) acts as a lyotropic template, whereas the second surfactant is an amphiphilic block copolymer (PE/B-b-PEO) that stabilizes the droplets. For template removal, the final material was calcined. The obtained materials were characterized by dynamic light scattering (DLS), transmission electron microscopy (TEM), scanning electron microscopy (SEM), atomic force microscopy (AFM), X-ray diffraction (XRD), and nitrogen sorption (Brunauer–Emmett–Teller (BET) methodology). The effect of synthesis conditions such as the amount of templating surfactant (CTAB), the temperature during ultrasonication, the reaction time, the pH value, and the amount of stabilizing surfactant (PE/B-b-PEO) on cooperative self-assembly, morphology, and specific surface area were investigated. Shortly after ultrasonication, porous particles a few hundreds of nanometers in size are formed, which are transformed to capsules and finally to porous flakes with increasing reaction time. This transformation is strongly influenced by the amount of stabilizing surfactant (PE/B-b-PEO). By simply varying the amount of PE/B-b-PEO, the morphology and mesostructural ordering, as well as the porosity, can be tuned over a wide range.

### Introduction

Mesoporous inorganic materials have attracted great interest, because of the variety of applications (for instance, as adsorption media, catalyst support, low-dielectric-constant fillers, drug delivery systems, and in the fields of chromatography, microelectronics or electro-optics).<sup>1,2</sup> Many methods have been established for the synthesis of mesoporous silica.<sup>3,4</sup> Most of the synthesis routes are based on either hydrothermal processing or sol–gel chemistry in combination with a templating approach. In the sol–gel process, appropriate precursors, mostly alkoxides are

transformed to silica by hydrolysis and condensation in an aqueous phase. After the reaction, the template must be removed by calcination or extraction. As a templating system, not only can single molecules be used<sup>5</sup> but also lyotropic phases, such as supramolecular assemblies of amphiphilic molecules (e.g., cetyltrimethylammonium bromide<sup>6</sup> (CTAB, used in the original synthesis of MCM-41)<sup>7</sup> or block co-polymers<sup>8</sup> in an adequate solvent, mostly water). This assembly serves as a template for mesophase

- \*.
- (1) Ying, J. Y.; Mehnert, C. P.; Wong, M. S. Synthesis and Applications of Supramolecular-Templated Mesoporous Materials. *Angew. Chem., Int. Ed.* **1999**, 38(1–2), 56–77.
  - (2) Lin, Y.-S.; Tsai, C.-P.; Huang, H.-Y.; Kuo, C.-T.; Hung, Y.; Huang, D.-M.; Chen, Y.-C.; Mou, C.-Y. Well-Ordered Mesoporous Silica Nanoparticles as Cell Markers. *Chem. Mater.* **2005**, 17(18), 4570–4573.
  - (3) Göltner, C. G.; Antonietti, M. Mesoporous Materials by Templating of Liquid Crystalline Phases. *Adv. Mater.* **1997**, 9(5), 431–436.
  - (4) Wan, Y.; Zhao, D. On the Controllable Soft-Templating Approach to Mesoporous Silicates. *Chem. Rev.* **2007**, 107(7), 2821–2860.

- (5) Iskandar, F.; Mikrajuddin; Okuyama, K. Controllability of Pore Size and Porosity on Self-Organized Porous Silica Particles. *Nano Lett.* **2002**, 2(4), 389–392.
- (6) Huo, Q.; Margolese, D. I.; Ciesla, U.; Demuth, D. G.; Feng, P.; Gier, T. E.; Sieger, P.; Firouzi, A.; Chmelka, B. F.; Schüth, F.; Stucky, G. D. Organization of Organic Molecules with Inorganic Molecular Species into Nanocomposite Biphase Arrays. *Chem. Mater.* **1994**, 6(8), 1176–1191.
- (7) Beck, J. S.; Vartuli, J. C.; Roth, W. J.; Leonowicz, M. E.; Kresge, C. T.; Schmitt, K. D.; Chu, C. T.-W.; Olson, D. H.; Sheppard, E. W.; McCullen, S. B.; Higgins, J. B.; Schlenker, J. L. A New Family of Mesoporous Molecular Sieves Prepared with Liquid Crystal Templates. *J. Am. Chem. Soc.* **1992**, 114(27), 10834–10843.
- (8) Andersson, N.; Kronberg, B.; Corkery, R.; Alberius, P. Combined Emulsion and Solvent Evaporation (ESE) Synthesis Route to Well-Ordered Mesoporous Materials. *Langmuir* **2007**, 23(3), 1459–1464.

formation. The water-soluble monomer is first dissolved and finally condensed in the water-rich, hydrophilic domains.

Beck et al.<sup>7</sup> suggested two principally different mechanisms for the synthesis of mesoporous silica. The first one assumes that a preformed water/surfactant liquid-crystal phase exists prior to the addition of the hydrolyzable and condensable inorganic precursor ("true liquid-crystal templating mechanism"). For this approach, the concentration of the templating surfactant is very high. The second mechanism proposes that the surfactant mesophase is only formed after the addition of the silica source ("cooperative self-assembly templating mechanism"). Here, the initial surfactant concentrations are much lower than the concentrations where lyotropic phases are formed; therefore, interactions between template and silica species are supposed to lead cooperatively to the formation of a liquid-crystal phase. This means that polymerization and formation of a lyotropic phase occurs simultaneously; therefore, control of the structure formation is a complex process.<sup>6,9</sup>

One of the major problems in the synthesis of mesoporous materials is the balance between the hydrolysis–condensation reactions on the one hand and the self-assembly process on the other. The crucial factors for cooperative self-assembly and morphology are the stability, the specificity, and the degree of organization of the template, which are dependent on the temperature, pH value, shape of surfactant micelles, counterions, ionic strength, and any other co-solvents present in the system.<sup>4,6,10,11</sup> Other important factors are the reactivity of the precursor and the water:precursor ratio.<sup>8</sup> By optimizing the precursor chemistry and processing conditions, materials with different structures and morphologies can be obtained.<sup>10,12</sup> Among all different morphologies that could be synthesized, mesoporous spherical nanoparticles are of considerable interest, because they can be used in many medical and biological fields, such as drug delivery or cell markers.<sup>2</sup> Mesoporous particles ~100 nm in size and with a specific surface area of ~900 m<sup>2</sup>/g could be synthesized in basic media at elevated temperature (80 °C).<sup>13</sup> Grün et al.<sup>14</sup> produced spherical particles with MCM-41 structure in a broad size range

(400–1100 nm, under basic conditions) by a modified cationic surfactant templating route. Specific surface areas of > 1000 m<sup>2</sup>/g could be obtained. Monodisperse spherical particles with a highly hexagonal structure in the size range of 490–680 nm could be synthesized.<sup>15</sup> The material showed a specific surface area up to 1200 m<sup>2</sup>/g; however, a large amount of surfactant had to be used. Another group reported the synthesis of mesoporous particles ~200 nm in size, using a time-consuming double-templating route.<sup>16</sup> Most of these syntheses occur under basic conditions and at elevated temperature (~100 °C).

Beneath all the syntheses of mesoporous nanoparticles, the synthesis of hollow mesoporous silica capsules has been the subject of many recent publications in materials science, because of their positive properties, such as a large specific surface area (> 500 m<sup>2</sup>/g) and surface permeability. Hollow capsules represent a distinct class of materials that can be used in the field of encapsulation for the controlled release of drugs, cosmetics, or dyes.<sup>17</sup>

For the synthesis of hollow particles many templates have been used. Usually, latex particles are used to fabricate larger cores (submicrometer to micrometer) and micelles are used for smaller cores (< 100 nm in size). In most publications, the colloidal particle templating is reported.<sup>17,18</sup> In the first step, core–shell particles are synthesized, e.g., by controlled surface precipitation of the precursor. In the second step, the core is removed by calcination at high temperatures or by extraction.<sup>17–20</sup> However, many of these methods are more complicated, with regard to the conditions for shell coating and core removal than other methods with liquid cores, such as emulsion,<sup>8,21,22</sup> or vesicles.<sup>23</sup>

Schacht et al.<sup>21</sup> first demonstrated that mesoporous ordered hollow spheres in the micrometer range can be synthesized by interfacial reactions in (oil-in-water) emulsions using CTAB as the templating surfactant under acidic conditions. Zoldesi et al.<sup>22</sup> synthesized hollow

- (9) Monnier, A.; Schüth, F.; Huo, Q.; Kumar, D.; Margolese, D.; Maxwell, R. S.; Stucky, G. D.; Krishnamurty, M.; Petroff, P.; Firouzi, A.; Janicke, M.; Chmelka, B. F. Cooperative Formation of Inorganic–Organic Interfaces in the Synthesis of Silicate Mesoporous Structures. *Science* **1993**, *261*(5126), 1299–1303.
- (10) Zhao, D.; Sun, J.; Li, Q.; Stucky, G. D. Morphological Control of Highly Ordered Mesoporous Silica SBA-15. *Chem. Mater.* **2000**, *12*(2), 275–279.
- (11) Rana, R. K.; Mastai, Y.; Gedanken, A. Acoustic Cavitation Leading to the Morphosynthesis of Mesoporous Silica Vesicles. *Adv. Mater.* **2002**, *14*(19), 1414–1418.
- (12) Zoldesi, C. I.; Imhof, A. Synthesis of Monodisperse Colloidal Spheres, Capsules, and Microballoons by Emulsion Templating. *Adv. Mater.* **2005**, *17*(7), 924–928.
- (13) Cai, Q.; Luo, Z.-S.; Pang, W.-Q.; Fan, Y.-W.; Chen, X.-H.; Cui, F.-Z. Dilute Solution Routes to Various Controllable Morphologies of MCM-41 Silica with a Basic Medium. *Chem. Mater.* **2001**, *13*(2), 258–263.
- (14) Grün, M.; Lauer, I.; Unger, K. K. The Synthesis of Micrometer- and Submicrometer-Size Spheres of Ordered Mesoporous Oxide MCM-41. *Adv. Mater.* **1997**, *9*(3), 254–257.

- (15) Yano, K.; Fukushima, Y. Synthesis of Mono-Dispersed Mesoporous Silica Spheres with Highly Ordered Hexagonal Regularity Using Conventional Alkyltrimethylammonium Halide as a Surfactant. *J. Mater. Chem.* **2004**, *14*, 1579–1584.
- (16) Chae, W.-S.; Braun, P. V. Templated Mesoporous Silica Colloids with Controlled Internal Structures. *Chem. Mater.* **2007**, *19*(23), 5593–5597.
- (17) Caruso, F.; Caruso, R. A.; Möhwald, H. Nanoengineering of Inorganic and Hybrid Hollow Spheres by Colloidal Templating. *Science* **1998**, *282*(5391), 1111–1114.
- (18) Chen, M.; Wu, L.; Zhou, S.; You, B. A Method for the Fabrication of Monodisperse Hollow Silica Spheres. *Adv. Mater.* **2006**, *18*(6), 801–806.
- (19) Lu, Y.; McLellan, J.; Xia, Y. Synthesis and Crystallization of Hybrid Spherical Colloids Composed of Polystyrene Cores and Silica Shells. *Langmuir* **2004**, *20*(8), 3464–3470.
- (20) Velikov, K. P.; van Blaaderen, A. Synthesis and Characterization of Monodisperse Core-Shell Colloidal Spheres of Zinc Sulfide and Silica. *Langmuir* **2001**, *17*(16), 4779–4786.
- (21) Schacht, S.; Huo, Q.; Voigt-Martin, I. G.; Stucky, G. D.; Schüth, F. Oil–Water Interface Templating of Mesoporous Macroscale Structures. *Science* **1996**, *273*(5276), 768–771.
- (22) Zoldesi, C. I.; Steegstra, P.; Imhof, A. Encapsulation of emulsion droplets by organo-silica shells. *J. Colloid Interface Sci.* **2007**, *308*(1), 121–129.
- (23) Hubert, D. H. W.; Jung, M.; Frederik, P. M.; Bomans, P. H. H.; Meuldijk, J.; German, A. L. Vesicle-Directed Growth of Silica. *Adv. Mater.* **2000**, *12*(17), 1286–1290.

particles with different shapes as spheres, microcapsules, and microballons by encapsulating emulsion droplets (oil-in-water) with a solid shell. However, the synthesis process is very time-consuming (up to 10 days). Rana et al.<sup>11</sup> synthesized hollow mesoporous particles between 50 and 500 nm with the use of CTAB and tetraethoxysilane (TEOS) in basic media. They obtained a specific surface area of 940 m<sup>2</sup>/g after calcination, but solid particles < 50 nm in size were additionally obtained with this synthesis route. Lu et al.<sup>24</sup> used the evaporation-induced self-assembly (EISA) technique to produce particles of ~200 nm. Here, a special aerosol deposition technique with a tubular reactor was used.

The disadvantage of most of these routes is that the spheres have either a wide size distribution or the morphology was not uniform. Moreover, the material is often not stable during calcination or washing. Most of the applications, however, require a stable structure and morphology. Because the pore structure, pore size, particle size, and particle morphology strongly influence the material's properties, it is important to tune all these parameters independently. However, control over architecture and morphology in an inorganic oxidic material is still a challenge, although much effort has been devoted to optimization procedures recently.<sup>25,26</sup>

To overcome the difficulties of the aforementioned methods and to achieve control over the morphology, we use the inverse miniemulsion technique, which is a very suited technique for the controlled synthesis of nanoparticles. This technique was already successfully used to synthesize mesoporous titania nanoparticles.<sup>27</sup> An inverse miniemulsion consists of aqueous nanodroplets that are homogeneously dispersed in an organic liquid. Unlike a microemulsion in which diffusion processes occur, leading to a fast exchange of reactants, a miniemulsion is stabilized against diffusion by the osmotic agent and is critically stabilized against coalescence and collision by surfactants. The process of miniemulsion is advantageous, because each droplet acts as an independent nanoreactor under preservation of droplet size, droplet number, and concentration in each droplet. Therefore, the final particle size can be easily tuned by the droplet size.<sup>28,29</sup>

A big challenge is the performance of the sol-gel chemistry and the cooperative self-assembly, in combination with the miniemulsion process to obtain structured

nanoparticles. The amphiphiles now serve several different functions:

(a) The self-assembly process of surfactant and inorganic precursors determines the final porous materials structure and is very sensitive toward external parameters.

(b) In addition, the amphiphiles serve as stabilizing agent for the miniemulsion droplets in a heterophase system.

In most of the synthesis protocols, alkoxides, such as tetramethoxysilane and TEOS are used as precursors. They are poorly water-soluble; therefore, an organic solvent as methanol or ethanol must be added. However, alcohols such as ethanol are detrimental to many lyotropic phases, because they increase the lipophilicity of the solvent, which changes the critical micelle concentration (cmc) of the surfactant. In addition, they influence the miniemulsion formation. The higher lipophilicity of the solvent results in a better solvatization of the hydrophobic parts of the surfactant and, consequently, the interactions between hydrophilic and hydrophobic parts are weakened.<sup>30</sup> Therefore, the synthesis of highly ordered materials is challenging in the confined space of a heterophasic miniemulsion system.

Hoffmann et al.<sup>31</sup> reported a glycol-modified precursor (tetrakis(2-hydroxyethyl)orthosilicate, EGMS) that is water-soluble. Because ethylene glycol is much better compatible with the self-assembly of silica species and liquid crystal phase than ethanol or methanol,<sup>32</sup> EGMS can be dissolved in the aqueous phase without the addition of a homogenizing co-solvent, such as ethanol, resulting in a simplified synthetic route. Glycol-modified silanes have already been used successfully to synthesize hierarchically structured (organo)silica monoliths.<sup>30,32</sup> Nevertheless, there are only very few reports concerning the use of EGMS as a precursor for the preparation of mesoporous silica particles.<sup>33</sup>

In this work, we combine the inverse miniemulsion technique with the sol-gel process and the cooperative self-assembly templating. This novel synthesis route results in porous silica materials with different controlled morphologies and high specific surface area. We observed the transformation of mesoporous particles into mesoporous capsules. This process can be tuned by adjusting the synthesis parameters, such as surfactant concentration and reaction time. As the structuring surfactant, we use CTAB, as in the original work by Beck.<sup>7</sup> In contrast to his work, we use concentrated acidic conditions at room temperature, with low surfactant concentrations (5 and

- (24) Lu, Y.; Fan, H.; Stump, A.; Ward, T. L.; Rieker, T.; Brinker, C. J. Aerosol-assisted self-assembly of mesostructured spherical nanoparticles. *Nature* **1999**, 398(6724), 223–226.
- (25) Fowler, C. E.; Khushalani, D.; Lebeau, B.; Mann, S. Nanoscale Materials with Mesostructured Interiors. *Adv. Mater.* **2001**, 13(9), 649–652.
- (26) Nooney, R. I.; Thirunavukkarasu, D.; Chen, Y.; Josephs, R.; Ostafin, A. E. Synthesis of Nanoscale Mesoporous Silica Spheres with Controlled Particle Size. *Chem. Mater.* **2002**, 14(11), 4721–4728.
- (27) Rossmanith, R.; Weiss, C. K.; Geserick, J.; Hüsing, N.; Hörmann, U.; Kaiser, U.; Landfester, K. Porous Anatase Nanoparticles with High Specific Surface Area Prepared by Miniemulsion Technique. *Chem. Mater.* **2008**, 20(18), 5768–5780.
- (28) Landfester, K. Polyreactions in Miniemulsions. *Macromol. Rapid Commun.* **2001**, 22(12), 896–936.
- (29) Landfester, K. Synthesis of Colloidal Particles in Miniemulsions. *Annu. Rev. Mater. Res.* **2006**, 36(1), 231–279.

- (30) Brandhuber, D.; Torma, V.; Raab, C.; Peterlik, H.; Kulak, A.; Hüsing, N. Glycol-Modified Silanes in the Synthesis of Mesoscopically Organized Silica Monoliths with Hierarchical Porosity. *Chem. Mater.* **2005**, 17(16), 4262–4271.
- (31) Sattler, K.; Hoffmann, H. A Novel Glycol Silicate and Its Interaction with Surfactant for the Synthesis of Mesoporous Silicate. In *Trends in Colloid and Interface Science XIII*; Springer: Berlin/Heidelberg, 1999; Vol. 112, pp 40–44.
- (32) Hüsing, N.; Brandhuber, D.; Kaiser, P. Glycol-Modified Organosilanes in the Synthesis of Inorganic-Organic Silsesquioxane and Silica Monoliths. *J. Sol-Gel Sci. Technol.* **2006**, 40(2–3), 131–139.
- (33) Geserick, J.; Hüsing, N.; Rossmanith, R.; Weiss, C. K.; Landfester, K.; Denkwitz, Y.; Behm, R. J.; Hörmann, U.; Kaiser, U. Mesoporous Silica and Titania by Glycol-modified Precursors. *Mater. Res. Soc. Symp. Proc.* **2007**, 1007, 1007-S04–1007-S13.



10 mol %, relative to the precursor), and a short synthesis time of only a few hours. The influence of the amount of templating surfactant (CTAB) and the temperature during ultrasonication on mesostructural ordering were investigated. The morphology could be tuned in a wide range by variation of the pH value and the amount of stabilizing block copolymer surfactant (poly((ethylene-co-butylene)-b-(ethylene oxide)), or PE/B-b-PEO).

### Experimental Part

**Materials.** Tetrahydrofuran (THF) (Merck, 99.8%) was distilled over sodium hydride prior to use. All other chemicals were used without further purification: TEOS (Merck, 99.9%), hydrochloric acid (1 M, Merck), sodium hydroxide (1 M, Merck), ethylene glycol (EG) (Merck, 99.5%), Isopar M (Caldic), cetyltrimethylammonium bromide (CTAB) (Fluka) and acetone (Merck, 99%). PE/B-b-PEO ( $M_w = 12\,000$  g/mol) was prepared by coupling "Kraton liquid" ( $\omega$ -hydroxypoly(ethylene-co-butylene),  $M_w = 3900$  g/mol) with ethylene oxide by anionic polymerization.<sup>34</sup> Demineralized water was used during the experiments.

**Synthesis of the Precursor.** EGMS was synthesized according to Mehrotra et al.<sup>35</sup> TEOS and ethylene glycol (EG) were reacted in a molar ratio of 1:4 in an argon atmosphere at 140 °C. Ethanol, which was produced during the transesterification, was removed continuously by distillation. Excess ethanol and TEOS were removed under vacuum. The synthesized glycol-modified precursor was characterized by thermogravimetric analysis (TGA): 9.7 wt % Si.

**Synthesis of SiO<sub>2</sub>.** Porous silica materials were prepared by the inverse miniemulsion technique. First of all, CTAB (5 and 10 mol %, relative to EGMS) was dissolved in 8.867 mL of aqueous phase (HCl/NaOH) of different pH (0, 4, 7, 10). Then, 307 mg of EGMS was added and the dispersed phase was mixed with the continuous organic phase that contained the stabilizing surfactant (PE/B-b-PEO, 0.7, 2.0, and 5.0 wt %, relative to the dispersed phase) and Isopar M (28 g). In the case of pre-emulsification, the dispersed phase was added to the continuous phase by stirring the system for 4 min under ice cooling. The mixed phases (a macroemulsion) were sonicated (Branson Model W-450 sonifier digital,  $\frac{1}{2}$  in. tip) in an ice-cooled bath at 90% amplitude for 30 s or 1 min (10 s pulse, 5 s pause). The reaction was performed at room temperature. The material was recovered by centrifugation, different times after ultrasonication and purified by repetitive centrifugation/redispersion using demineralized water and acetone. The resulting silica was dried in air, followed by calcination at 600 °C for 3 h.

**Characterization.** The average size of the droplets was measured using a Zetasizer Nano Series (Malvern Instruments, U.K.) at a fixed scattering angle of 173°. Dynamic light scattering (DLS) measurements give a value called Z-average size, which is an intensity average, and the polydispersity index. The standard cumulant analysis is the fit of a polynomial to the logarithm of the correlation function (G1) (see eq 1).

$$\ln(G1) = a + bt + ct^2 + dt^3 + \dots \quad (1)$$

The value of second-order cumulant  $b$  is converted to a size using the dispersant viscosity and some instrumental constants. The

coefficient of the squared term  $c$ , when scaled as  $2c/b^2$ , is known as the polydispersity (or the polydispersity index, PDI). The calculations for these parameters are defined in ISO Standard Document 13321:1996 E.

The particle size and morphology were determined by transmission electron microscopy (TEM) (Philips Model EM 400T) and scanning electron microscopy (SEM) (Zeiss Model DSM 962 instrument). One droplet of the miniemulsion was placed on a carbon-coated copper grid for TEM. The silica powders were dispersed in acetone previously. For SEM, one droplet was placed on an aluminum plate, and the samples were dried at room temperature; with TEM analysis, the grid was examined at an accelerating voltage of 80 kV without additional contrasting. Before examination with SEM, the aluminum plates were sputtered with Pd/Au.

For atomic force microscopy (AFM), one droplet of the miniemulsion was placed on a silicon plate and dried by spin coating.

The crystalline phase was identified by X-ray diffraction (XRD) using Cu K $\alpha$  radiation ( $\lambda = 0.154$  nm) on a PANalytical Xpert Pro. The specific surface area of the material was determined by nitrogen sorption experiments on an Autosorb MP1 instrument (Quantachrome). The surface area was calculated by the five-point method, according to the Brunauer–Emment–Teller (BET) methodology, in the  $p/p_0$  range of 0.05–0.3. Prior to the measurement, the samples were degassed at 150 °C for 3 h in vacuo.

### Results and Discussion

The focus of this work relies on the synthesis of mesoporous silica particles and capsules with high specific surface area. These materials have been prepared by sol–gel processing of a glycol-modified silane (tetrakis(2-hydroxyethyl)orthosilicate, EGMS) in miniemulsion. Via hydrolysis and condensation, silica is formed under the release of ethylene glycol. EGMS shows the advantage of being highly water-soluble. With the use of this precursor, the structuring surfactant can be directly dissolved in the aqueous phase without the addition of another solvent (such as ethanol), which might destabilize the miniemulsion. This allows a convenient handling in miniemulsion. For the synthesis, an inverse miniemulsion process is used. Because we already successfully produced other mesoporous inorganic oxides (TiO<sub>2</sub>) in miniemulsion,<sup>27</sup> we started the preparation of silica with a similar system and related synthesis conditions. The precursor (EGMS) and the structuring surfactant (CTAB) were dissolved in hydrochloric acid and dispersed in a mixture of linear, long-chain hydrocarbons (Isopar M). Via homogenization using ultrasonication, stable droplets in the several-hundred-of-nanometers size range were formed. In this synthesis, two different surfactants were used. One surfactant (CTAB) is soluble in the dispersed, aqueous phase and acts as lyotropic template for the inorganic material, whereas the second surfactant is an amphiphilic block co-polymer (PE/B-b-PEO), dissolved in the continuous organic phase, stabilizing the droplets sterically against droplet collision and coalescence. The process of miniemulsion is advantageous because it produces small (100–1000 nm) homogeneous droplets in which hydrolysis and condensation to the final silica

(34) Thomas, A.; Schlaad, H.; Smarsly, B.; Antonietti, M. Replication of Lyotropic Block Copolymer Mesophases into Porous Silica by Nanocasting: Learning about Finer Details of Polymer Self-Assembly. *Langmuir* **2003**, *19*(10), 4455–4459.

(35) Mehrotra, R. C.; Narain, R. P. Reactions of Tetramethoxy- & Triethoxysilanes with Glycols. *Indian J. Chem.* **1967**, *5*(9), 444.

material occur. For template removal, the material was calcined.

In the following, the effect of synthesis conditions such as the amount of templating surfactant (CTAB), the temperature during ultrasonication, the reaction time, the pH value, and the amount of stabilizing surfactant (PE/B-b-PEO) on cooperative self-assembly, morphology, and specific surface area were investigated. For characterization of the obtained material, dynamic light scattering (DLS), transmission electron microscopy (TEM), and scanning electron microscopy (SEM), atomic force microscopy (AFM), X-ray diffraction (XRD), and nitrogen sorption (BET methodology) were used.

**Conditions for a Stable Miniemulsion and Mesostructural Ordering.** Because large quantities of PE/B-b-PEO resulted in less and even no structuring of the obtained silica, the concentrations of PE/B-b-PEO used here were set as sufficient to give reasonable stable miniemulsions but low enough to avoid significant dissolution of surfactant in the droplet phase. The minimum quantity of PE/B-b-PEO was determined to be 0.7 wt %, with respect to the dispersed phase. Lower amounts of surfactant could not stabilize the miniemulsion and led to immediate phase separation.

Another crucial parameter for mesostructural ordering is the energy input into the system that is necessary to form the droplets. A low energy input is not sufficient for efficient homogenization, but if the energy input becomes too high, mesostructure formation is inhibited. Thus, the amplitude as well as the time of ultrasonication, which determines the energy input, had to be adjusted. Because even 5 min of reduced amplitude (70% and 80%) was not sufficient for homogenization of the miniemulsion system, an amplitude of 90% was required. With 1 min of ultrasonication and 10 mol % CTAB (in ratio to EGMS), a stable miniemulsion system could be obtained. As the concentration of stabilizing surfactant is at the lower limit (0.7 wt %, with respect to the dispersed phase), the obtained droplet sizes were  $\sim 900$  nm in diameter with PDI values of  $\sim 0.4$ . With these reaction conditions and via centrifugation of the miniemulsion after 4 h of synthesis, mesostructural ordering in the inorganic particles was achieved as can be seen in the XRD pattern (see Figure 1). After calcination for template removal, one broad reflection (100) was obtained corresponding to a  $d$ -spacing of 4.2 nm showing that the sample has a uniform ordered pore structure. This value is consistent with the pore size of 3.8 nm that was obtained by Beck et al.,<sup>7</sup> using CTAB. However, the (110) and (200) reflections that would be expected for long-range hexagonal ordering were not observed. A most likely reason for the absence of these higher-order reflections might be the lack of large diffraction domains, which is especially the case in small nanoparticles, as can be seen in the TEM images (see Figure 2a). Silica nanoparticles 50–100 nm in size (see Figure 2a) were synthesized as well as very thin, folded sheets in the micrometer range (namely, flakes) showing highly ordered hexagonal arrays (see Figure 2b). The diffraction domains in these big flakes are extremely

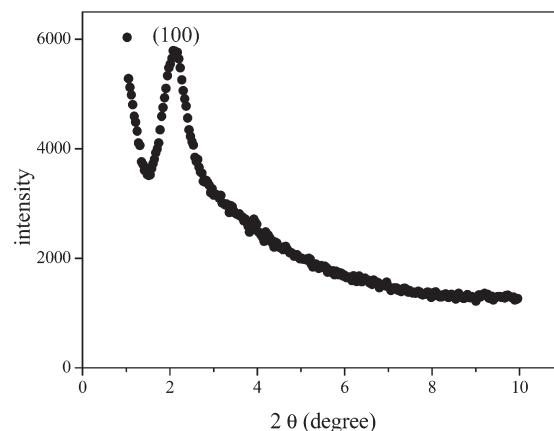


**Figure 1.** XRD pattern of the obtained material synthesized with 10 mol % CTAB (calcined at 600 °C).

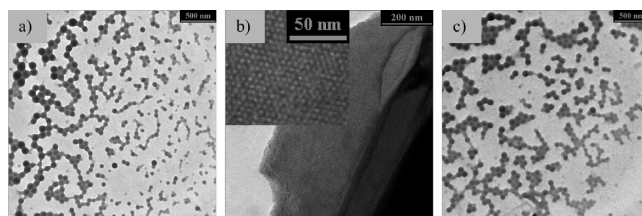


**Figure 2.** TEM images of (a) silica nanoparticles 50–100 nm in size, synthesized with 10 mol % CTAB, (b) a hexagonally ordered silica flake synthesized with 10 mol % CTAB, and (c) silica nanoparticles  $\sim 100$  nm in size, synthesized with 5 mol % CTAB. All samples were calcined at 600 °C.

large; therefore, they will mainly contribute to the X-ray reflection.

To explain the mesostructural ordering, we assume that a cooperative self-assembly mechanism occurs. In a CTAB water solution without the addition of silica, the transformation from micelles to a hexagonal liquid-crystal phase occurs at  $\sim 28$  wt % at room temperature.<sup>36</sup> Because we worked far below this concentration, the mesostructure formation and thus self-assembly is driven by the presence of silica oligomers via the formation of strong multidentate linkages to the template.<sup>26</sup> Because we are working under acidic conditions with a cationic surfactant, the inorganic species ( $-\text{Si}-\text{OH}_2^+$ ), as well as the surfactant, have the same charge. In this case, halogen anions are acting as a mediator of opposite charge ( $\text{S}^+\text{X}^-\text{I}^+$ ).<sup>6,37</sup>

To investigate the influence of CTAB concentration on the mesostructural ordering, the CTAB concentration was varied. With 5 mol %, and as well as 10 mol %, CTAB (in ratio to EGMS), the final material contained nanoparticles (see Figure 2c) and structured flakes in the micrometer range. For the latter amount of surfactant, the particles were slightly bigger ( $\sim 100$  nm) and structuring was also obtained, as could be shown by XRD

- (36) Choudhury, S. R.; Yadav, R.; Maitra, A. N.; Jain, P. C. Structural Transformations in CTAB Aggregated Systems Investigated by Positron Lifetime Spectroscopy. 1. Binary Systems. *Colloids Surf. A* **1994**, 82(1), 49–58.
- (37) Huo, Q.; Margolese, D. I.; Ciesla, U.; Feng, P.; Gier, T. E.; Sieger, P.; Leon, R.; Petroff, P. M.; Schüth, F.; Stucky, G. D. Generalized Synthesis of Periodic Surfactant/Inorganic Composite Materials. *Nature* **1994**, 368(6469), 317–321.

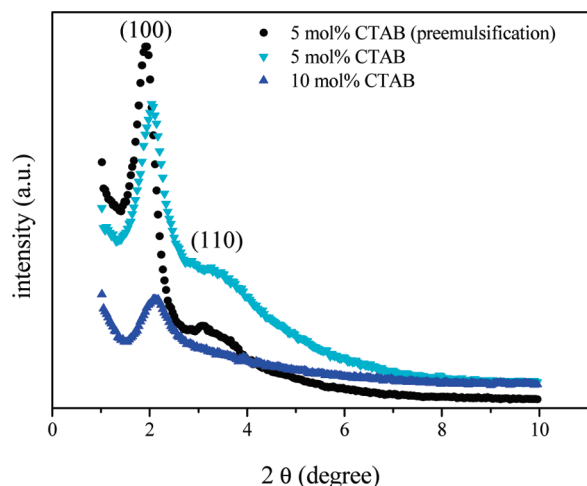


**Figure 3.** XRD patterns of silica synthesized with different amount of CTAB: 10 mol % CTAB (dark blue curve), 5 mol % CTAB (light blue curve), and 5 mol % CTAB with pre-emulsification (black curve). All samples were calcined at 600 °C.

(see Figure 3). The droplet sizes of the miniemulsion increased to  $\sim 1700$  nm for 5 mol % CTAB with PDI values of  $\sim 0.3$ . As an amphiphilic molecule, CTAB is partly located at the interface between the dispersed aqueous and the continuous organic phase, thus contributing to a larger extent to the stabilization of the droplets.

Because the energy input is a crucial factor for mesostructure formation (as already mentioned previously), the ultrasonication time required for homogenization of the system with 5 mol % CTAB could be further reduced by preparing a macroemulsion before ultrasonication (pre-emulsification). Under these conditions, only 30 s of ultrasonication were sufficient to obtain a stable miniemulsion with droplet sizes of  $\sim 1800$  nm (which is slightly higher, compared to 1700 nm, obtained with an ultrasonication time of 1 min) and an unchanged PDI of 0.3.

Comparing the X-ray patterns of the different synthesis conditions (see Figure 3), the reflections become narrower and more intense with a lower amount of CTAB (5 mol % instead of 10 mol %) and with shorter ultrasonication time (30 s instead of 1 min, pre-emulsification), indicating a narrower pore size distribution. With 5 mol % CTAB, a second reflection between  $3.1^\circ$  and  $3.3^\circ$  ( $2\theta$ ) can be observed, which can be assigned to the (110) reflection of a hexagonal ordering. Silica with specific surface areas up to  $1800 \text{ m}^2/\text{g}$  could be obtained after calcination at 600 °C.

The amounts of PE/B-b-PEO and CTAB, and the ultrasonication time, play an important role for the stability of the miniemulsions and for mesostructural ordering, the optimized reaction conditions are a compromise between both stabilization and structuring of the final material.

**Temperature Control during Homogenization.** In the following section, the temperature during homogenization was varied. This is another possibility to control the energy input into the system. With decreasing temperature, the reaction rate, as well as the mobility of the surfactant molecules, are expected to decrease. Consequently, the conditions for cooperative self-assembly are

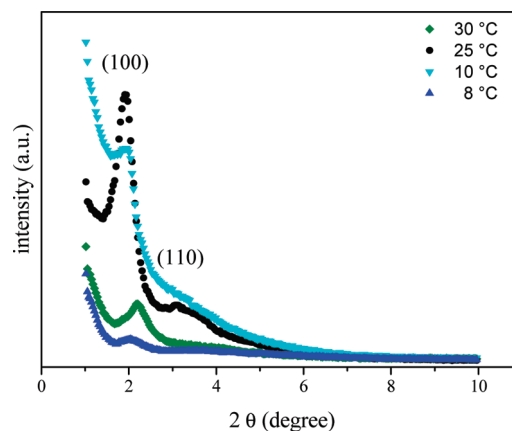


**Figure 4.** XRD patterns of silica synthesized with temperatures of 8 °C (dark blue curve), 10 °C (light blue curve), 25 °C (black curve), and 30 °C (green curve) during ultrasonication. All samples were calcined at 600 °C.

changed, and, therefore, the final structuring also can be influenced. In these syntheses, the systems did not exceed the adjusted temperatures during ultrasonication (8, 10, 25, and 30 °C). When the target temperature is reached, ultrasonication stops, the system cools (using an ice bath), and ultrasonication is continued until the preset temperature is reached again. To obtain a stable miniemulsion and prevent phase separation, the ultrasonication time for these experiments was increased to 1 min, because some of the chosen temperatures were quite low (8 and 10 °C), resulting in a short pulsing period of a few seconds. Temperatures of  $< 8$  °C were not possible, because the pulsing period was too short for homogenization. After ultrasonication, the miniemulsions were left at room temperature for reaction. The droplets of these emulsions were measured to be  $\sim 1500$  nm (DLS) with PDI values of  $< 0.3$ . As observed with TEM, the particles were  $\sim 100$  nm and the large flakes in the micrometer range. The particle size did not change with different temperatures.

Comparing the X-ray patterns (see Figure 4), the temperature during ultrasonication strongly influences the intensity of the (100) reflection at  $1.9^\circ$  ( $2\theta$ ). It becomes more pronounced, indicating a higher degree of structuring with increasing temperature. At a maximum temperature of 8 °C during ultrasonication, the X-ray pattern shows only a slight reflection after calcination. At 10 °C, a slight shoulder can be observed and a clear reflection can be detected only with 25 and 30 °C. Only at a temperature of 25 °C, the (100) reflection is very narrow and shows high intensity, and, additionally, even a second reflection (110) at  $3.1^\circ$  ( $2\theta$ ) can be observed. This is consistent with results that have been previously reported that room temperature is suitable to obtain mesostructural ordering and heating or cooling is not necessary as the rate of self-assembly of the surfactant as well as condensation of the siliceous species slows with decreasing temperature.<sup>4</sup> Therefore, the differences in the rates obviously lead to a disturbance in the cooperative self-assembly process.

The total ultrasonication time, as well as the temperature after ultrasonication, was the same for all these systems; therefore, the only difference lies in the temperature



during ultrasonication and, consequently, in the pulsing period. In the case of lower temperatures (8 and 10 °C), the preset temperature is already reached after a few seconds, and, therefore, the pulsing period is shorter, resulting in a longer total reaction time. In the case of a higher temperature (25 and 30 °C), it takes longer (several seconds) until the preset value is reached and ultrasonication stops; therefore, the pulsing period is longer as well, compared to only a few seconds. Thus, ultrasonication (as already mentioned) and, here, especially the pulsing period seem to be crucial factors for mesostructure formation.

Sonochemistry has already been used to prepare various mesoporous oxides and amorphous materials.<sup>38–40</sup> Suslick et al.<sup>38</sup> observed an increased reactivity induced by sonication. They explain this by the localized high temperatures that enhance the reaction rates. Indeed, for this demand, ultrasound is already used in many reactions.<sup>38</sup> Compared to our experiments, with a lower preset temperature (8 and 10 °C) during ultrasonication, the pulsing period is shorter (a few seconds), and, therefore, the reaction rate is not fast enough, compared to higher preset temperatures (25 and 30 °C) with longer pulsing periods (several seconds). Obviously, this reaction rate at the beginning at 8 and 10 °C is not fast enough to result in a mesostructural ordering of the material. Consequently, a fast reaction rate at the beginning synthesis step is apparently important to induce cooperative self-assembly.

Moreover, the absence of mesostructural ordering with low temperatures during ultrasonication also indicates that the condensation of the siliceous precursor to the final material occurs quite quickly. The cooperative self-assembly in the final product is influenced by the temperature during this short ultrasonication time, although, after ultrasonication, all the systems were left at room temperature for 4 h. This indicates that hydrolysis and condensation occur very fast under these synthesis conditions, determining the final structure of the material already in the first few minutes of synthesis, which means shortly after the precursor and CTAB are dissolved in the aqueous phase.

Comparing the X-ray reflections for 25 and 30 °C the one for 25 °C is narrower and shows higher intensity. Although a temperature of 30 °C favors cooperative self-assembly, because of sufficient mobility of the surfactant molecules, the pulsing period at this temperature is too long, resulting in reduced structure formation. To obtain mesostructural ordering, a compromise must be found between cooperative self-assembly, which is favored by increasing temperature, and the ultrasonication time,

which should be long enough to induce structuring by increasing the reaction rate, but short enough to avoid excessive energy input, which inhibits structure formation.

**Reaction Time.** As described previously, we obtained a mixture of particles and flakes after 4 h of reaction time. Thus, in further studies, we wanted to investigate when and how the formation of particles and flakes occurs, and, therefore, the reaction time was varied, keeping constant the amount of CTAB (5 mol %) and the temperature during ultrasonication (25 °C). The materials obtained after different times were examined by electron microscopy. Samples were taken out of the miniemulsion and dried in air. All time data indicated in the following sections were related to the time of ultrasonication, which was set as the zero point.

With a dispersed phase of pH 0, 15 min after ultrasonication, the sample consisted mainly of porous particles ~100 nm in size (see Figure 5a). Compared to the droplet sizes measured by DLS (~1700 nm), many small particles grow in one miniemulsion droplet. In addition to these particles, another type of particle was detected what we call “capsules”, which were ~200 nm in size (and even bigger). They seem to be hollow and partly collapsed, and they are randomly located between the particles. Investigations with high-resolution SEM (see Figures 5d and 5e) showed that the particle surface is not smooth and that the capsules are hollow and partially broken. One hour after ultrasonication, the sample mainly consisted of porous capsules and flakes of much bigger size (> 1 μm). After 2 h, the number of particles decreased further (see Figure 5b); after 4 h, mostly porous flakes ~2 μm in size were obtained. After one day, the same composition could be detected (see Figure 5c). Studies with atomic force microscopy (AFM) also revealed the same transformation process with time (see Figure 6).

This transformation process explains why we obtained a mixture of particles and flakes with a synthesis time of 4 h (see Figure 2). The reason why capsules could not be detected might be ascribed to the different sample treatments. As described previously, the particles were separated by centrifugation 4 h after ultrasonication and washed with water and acetone. Therefore, the already damaged and broken capsules might be transformed to flakes, because of the presence of water and silanol groups on the capsule surface. Consequently, only the remaining particles and flakes could be detected. The reason why mesostructured materials are only formed after 4 h might be explained like this. Fowler et al.<sup>25</sup> synthesized mesostructured nanoparticles < 100 nm in size in basic media. They obtained less-ordered nanoparticles after a short reaction time (neutralization and drying 1 min after mixing precursor and template) and structured particles after a longer time (neutralization and drying a few minutes after mixing precursor and template). They postulated that the disordered nanoparticles are favored kinetically while the structured nanoparticles are thermodynamically stable. Therefore, the latter are only formed after a longer reaction time.

(38) Suslick, K. S. Sonochemistry. *Science* **1990**, 247(4949), 1439–1445.

(39) Gedanken, A.; Tang, X.; Wang, Y.; Perkash, N.; Koltypin, Y.; Landau, M. V.; Vradman, L.; Herskowitz, M. Using Sonochemical Methods for the Preparation of Mesoporous Materials and for the Deposition of Catalysts into the Mesopores. *Chem.—Eur. J.* **2001**, 7(21), 4547–4552.

(40) Tang, X.; Liu, S.; Wang, Y.; Huang, W.; Sominski, E.; Palchik, O.; Koltypin, Y.; Gedanken, A. Rapid synthesis of high quality MCM-41 silica with ultrasound radiation. *Chem. Commun.* **2000**, 21, 2119–2120.

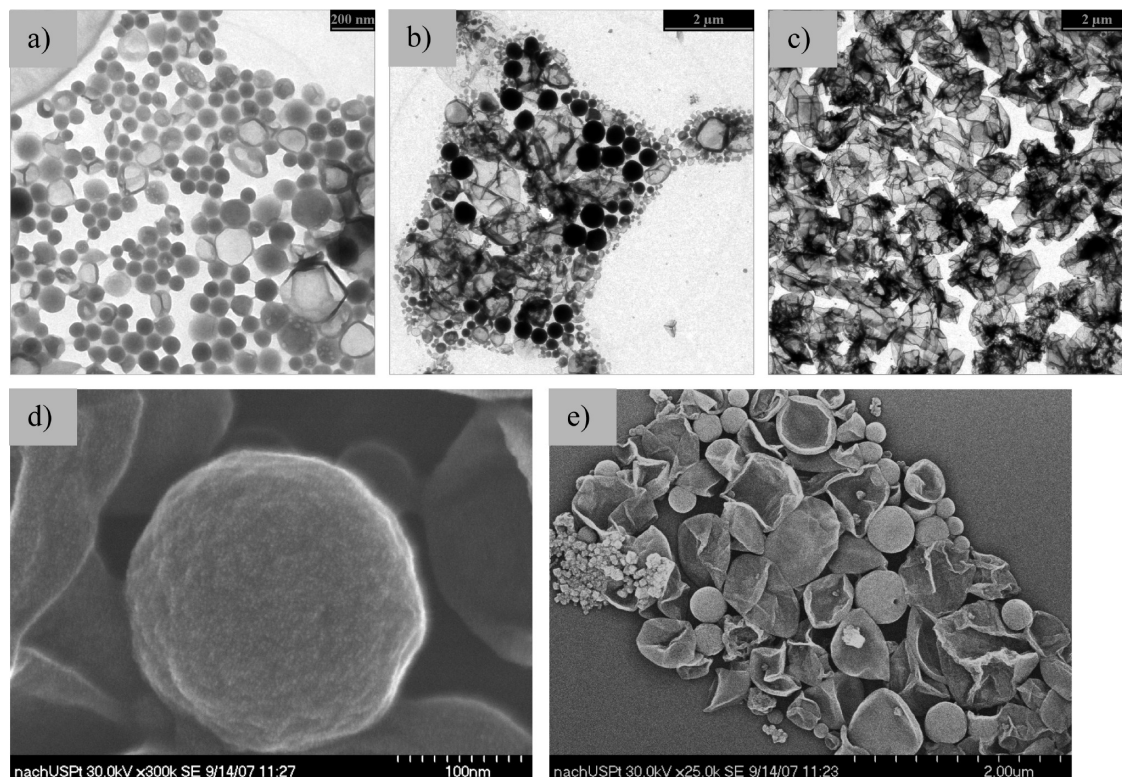


**Figure 5.** Electron microscopy images of porous silica particles, capsules, and flakes synthesized with a dispersed phase of pH 0. The samples have been taken 15 min (panels a, d, e), 2 h (panel b), and 1 d (panel c) after ultrasonication, without calcination and examined via (a–c) TEM and (d, e) SEM.

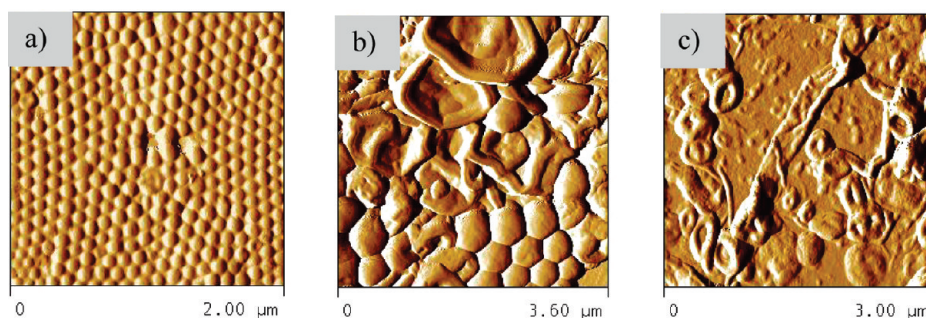


**Figure 6.** AFM images of silica particles, capsules, and flakes synthesized with a dispersed phase of pH 0. The samples have been taken (a) 15 min, 2 h (b) and 4 h (c) after ultrasonication without calcination.

**Variation of the pH Value.** In the following section, we investigated if the pH value of the dispersed phase influences the morphology of the final material, because the reaction rates of hydrolysis and polycondensation are strongly dependent on the pH value. As already mentioned, with a pH value of 0, the transformation of the precursor to silica seems to be quite fast. Therefore, with a lower reaction rate the morphology of the obtained silica might be changed.

With pH 4, we did not obtain any particles 15 min after ultrasonication. TEM images show big spherical hollow aggregates 1–4  $\mu\text{m}$  in size (see Figure 7a). They seem to be extremely thin and consist of folded and intergrown porous capsules. The size distribution was quite broad. With increasing time, the buildings grew and, after 1 d, mainly big flakes could be observed. With a neutral pH (pH 7) we obtained mainly porous spherical hollow aggregates (or filigrane hollow particles)  $\sim 2 \mu\text{m}$  in size

and few capsules  $\sim 200 \text{ nm}$  in size after 15 min (see Figure 7b). With increasing time, only large porous flakes could be observed. With pH 10, the final material was very similar to pH 7 (see Figure 7c). Spherical porous structures 1–2  $\mu\text{m}$  in size were formed, and, after one day, flakes could be detected. The different morphologies of silica obtained with different pH values of the dispersed phase are summarized in Table 1.

There are several factors that can influence the morphology of the final material, such as the hydrolysis and condensation rates, the shapes of surfactant micelles, the interactions between them, and the presence of additives in the system.<sup>4,10</sup> Here, with different pH values, the hydrolysis and condensation rates must be considered. The hydrolysis is catalyzed in acidic and basic media, which means the reaction rate shows a minimum at pH 7. The rate of condensation is minimal between pH 2 and pH 4, because the isoelectric point of silica is located at



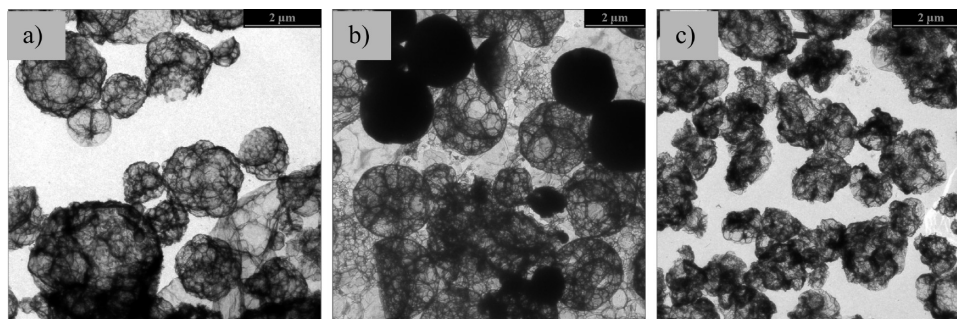


**Figure 7.** TEM images of silica with spherical hollow (or filigrane hollow) morphology synthesized with (a) pH 4, (b) pH 7, and (c) pH 10 of the dispersed phase. The samples have been taken 15 min after ultrasonication without calcination.

**Table 1. Different Morphologies of Silica Materials Obtained with Different pH Values of the Dispersed Phase**

pH value of the dispersed phase	morphology after 15 min
0	particles, few capsules
4	spherical hollow aggregates
7	spherical hollow aggregates, capsules
10	spherical hollow aggregates, few capsules

pH  $\sim 2$ .<sup>30,41</sup> Strongly acidic media accelerates both the hydrolysis and the condensation reaction with  $H^+$  ions as the catalyst. Therefore, after 15 min, silica particles are already formed and almost the entire amount of the precursor has already reacted. Because hydrochloric acid, as well as released ethylene glycol are present, in the droplets during particle formation, silica hard spheres as well as hollow particles can be formed that contain hydrochloric acid or ethylene glycol.

As shown in the literature, in parallel to the sol–gel process, phase separation occurs.<sup>32</sup> There are two different types. One type is the phase separation that results in mesopores by forming surfactant/silica assemblies (microphase separation) and the second type of phase separation, which is also termed polymerization-induced phase separation, leads to a macroscopic ordering by separation into a solvent-rich phase, which consists of water and ethylene glycol, and an organosilica/surfactant phase (macroscopic ordering). Both transformations are connected and determine the final structure.<sup>32,42</sup>

Hubert et al.<sup>23</sup> also observed the formation of similar morphologies as broken capsules during the reaction course. They explain this with the production of alcohol or the mechanical stress caused by the condensed growing silica network. This can also explain why the hollow capsules in our system collapsed with time. In many TEM images, small holes on the particle surface, as well as creases and folds (indicating the beginning of the collapse of the thin spherical shell), could be detected. Because there are  $OH^-$  groups on the particle surface and hydrochloric acid is still present in the system until the sample dried completely, further condensation of uncondensed surface groups of different broken spheres and capsules can proceed. Therefore, the

capsules grow together and form porous flakes of increasing size. As described in the literature, synthesis in acidic media is suitable to form mesoporous silica with a large variety of morphologies.<sup>41</sup> This is related to the different mechanisms of the hydrolysis and condensation reactions. If hydrolysis occurs in acidic media, more chain-like silica oligomers are generated, which can adopt a variety of different shapes.<sup>43</sup> The morphology is sometimes difficult to control, but spherical particles are usually the main product.<sup>4</sup>

If we work at pH 4, hydrolysis occurs relatively fast but condensation is rather slow. If samples are removed too early from the reaction vessel (e.g., 15 min after ultrasonication), the material is not stable, because the silica particles are not formed yet. There are still many noncondensed silica species that continue to condense and grow together, forming loose structures. Their size and spherical hollow shape is similar to the droplet sizes (1700 nm) measured by DLS after ultrasonication. During drying of the sample, the structures further grew together. At pH 7 and 10, it is difficult to explain the obtained morphologies with the reaction rates. Here, both processes occur simultaneously and are still continuing after 15 min as the morphologies are still changing with time. With both pH values, we obtained mostly spherical hollow aggregates after 15 min.

Eventually, the morphology of the final material is not only dependent on the reaction time but also on the pH value of the dispersed phase. Because we consider the applications for porous particles especially important (as already mentioned), we continued to perform further experiments at pH 0, because, at this pH, the greatest amount of particles could be obtained.

**Variation of the Concentration of PE/B-b-PEO.** The stabilizing surfactant PE/B-b-PEO can also act as a structure-directing agent.<sup>34,44</sup> In the aforementioned experiments, no templating effect by PE/B-b-PEO could be observed, because the obtained pores ( $\sim 4$  nm in size) were in the typical size range of CTAB.<sup>7</sup> To investigate the influence of the stabilizing surfactant on the particle morphology, the amount of PE/B-b-PEO was varied between 0.7 wt % and 5 wt %, relative to the dispersed phase.

(41) Lin, H.-P.; Mou, C.-Y. Structural and Morphological Control of Cationic Surfactant-Templated Mesoporous Silica. *Acc. Chem. Res.* **2002**, *35*(11), 927–935.

(42) Nakanishi, K. Pore Structure Control of Silica Gels Based on Phase Separation. *J. Porous Mater.* **1997**, *4*(2), 67–112.

(43) Yang, H.; Coombs, N.; Ozin, G. A. Morphogenesis of Shapes and Surface Patterns in Mesoporous Silica. *Nature* **1997**, *386*(6626), 692–695.

(44) Smarsly, B.; Grosso, D.; Brezesinski, T.; Pinna, N.; Boissière, C.; Antonietti, M.; Sanchez, C. Highly Crystalline Cubic Mesoporous  $TiO_2$  with 10-nm Pore Diameter Made with a New Block Copolymer Template. *Chem. Mater.* **2004**, *16*(15), 2948–2952.

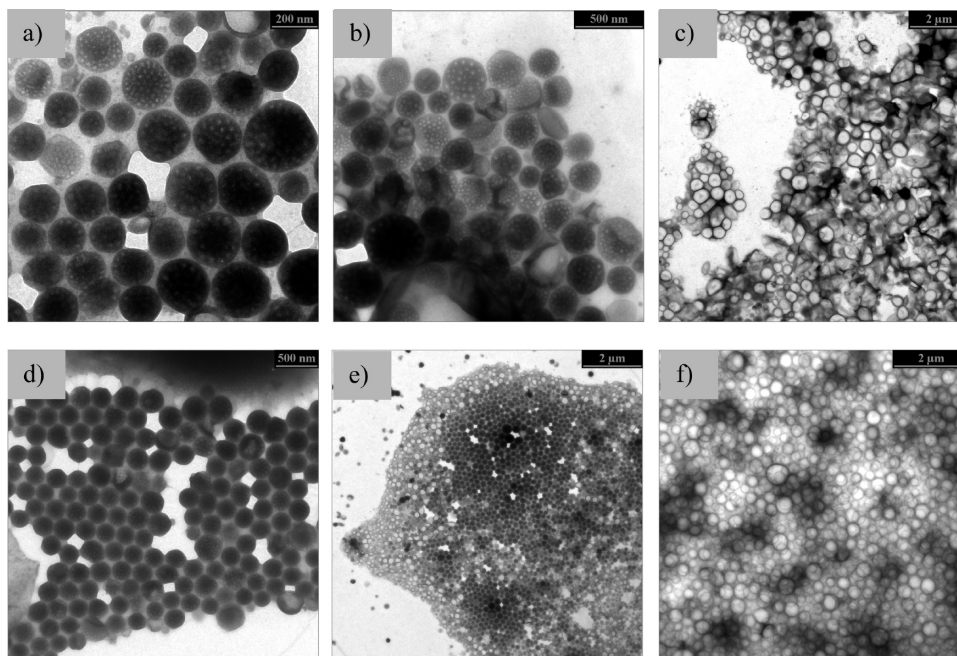


**Figure 8.** TEM images of porous silica particles and capsules synthesized with (a–c) 2 wt % and (d–f) 5 wt % PE/B-b-PEO, relative to the dispersed phase. Samples were obtained (a, d) 15 min, (b, e) 2 h, and (c, f) 1 d after ultrasonication without calcination.

**Table 2.** Average Droplet Size, Polydispersity Index (PDI), Morphology, and Specific Surface Area of the Samples Prepared with Different Amounts of PE/B-b-PEO

amount of PE/B-b-PEO (wt %)	droplet diameter (nm)	PDI	After 15 min of Ultrasonication		After 1 d of Ultrasonication	
			morphology	specific surface area [m <sup>2</sup> /g]	morphology	specific surface area [m <sup>2</sup> /g]
0.7	1813	0.374	particles, few capsules		flakes	
2.0	1049	0.222	mostly particles, few capsules	500–600	capsules, few particles	480–730
5.0	923	0.249	only particles		only capsules	

With 0.7 wt % PE/B-b-PEO, we obtained mainly porous particles after 15 min (see Figure 5a), as described previously. With 2 wt % PE/B-b-PEO, only very few capsules were obtained, while the remainder of the sample consisted of particles ~200 nm in size (Figure 8a) with higher porosity (TEM) and a larger pore size (13 nm, as determined via TEM), compared to the sample prepared with 0.7 wt % PE/B-b-PEO (4 nm in size). After 1 and 2 h (see Figure 8b), we observed a mixture of particles and capsules with the increasing amount of capsules. Compared to the synthesis with 0.7 wt % PE/B-b-PEO, no flakes were detected. After 4 h, the main portion of the sample consisted of capsules and after 1 d (see Figure 8c), mostly capsules in a broad size range (150–600 nm) and very few particles could be obtained. This broad size distribution indicates again that the capsules are presumably generated out of single hollow particles and then grew together by coalescence of capsules as silanol groups on the particle surface are still present.

When the amount of PE/B-b-PEO is further increased to 5 wt %, only homogeneous porous particles ~300 nm in size, with a pore size of ~13 nm (TEM), could be obtained after 15 min (see Figure 8d). After 1 h, a small amount of capsules could be detected; after 2 h, the sample consisted of a mixture of porous particles and

capsules (Figure 8e). One day after ultrasonication, the TEM images only show capsules (see Figure 8f), which were bigger and more homogeneous in size, compared to the synthesis with a smaller amount of PE/B-b-PEO. The sizes of the capsules are consistent with the droplet sizes after ultrasonication. One droplet seems to be transformed into one capsule after 24 h. The average droplet sizes, PDI values, morphologies, and specific surface areas of the samples prepared with different amounts of PE/B-b-PEO are summarized in Table 2.

This shows that the amount of PE/B-b-PEO influences the transformation of particles to capsules and flakes. Larger amounts of PE/B-b-PEO increase the stabilization of the particles and, therefore, slow the transformation to capsules. Because PE/B-b-PEO is an amphiphilic molecule and is soluble in the continuous, organic phase, the surfactant is located at the interface between the dispersed, aqueous phase and the continuous, organic phase. Its hydrophilic component, which consists of poly(ethylene oxide) chains, is partly inside the droplets. Consequently, the surfactant can interact with the silica species by hydrogen bonds between the OH– groups of the silica species and the ether oxygens of PEO. Therefore, it is possible that the precursor is also associated with the PEO of the template. As reported in

the literature,<sup>45,46</sup> such an interaction is especially observed at pH  $\sim$ 1. As we work with an aqueous phase of pH 0, this interaction will presumably occur and, therefore, PE/B-b-PEO can contribute to the particle stabilization. Moreover, PE/B-b-PEO can also enhance the porosity of the final material. The absence of a reflection in the XRD pattern in the small angle area is probably due to a lack of long-range order or disordered pore arrangements. With higher amounts of PE/B-b-PEO, pore sizes of  $\sim$ 13 nm (as observed via TEM) were obtained. This size range is similar to that reported by Smarsly et al.,<sup>34,44</sup> who already used this poly(ethylene oxide)-based surfactant for mesoporous ordering in the synthesis of porous silica and titania. Thus, the change in porosity, as well as the higher pore size of  $\sim$ 13 nm (compared to  $\sim$ 4 nm of CTAB), is attributed to PE/B-b-PEO. With different amounts of this surfactant the morphology, the mesoporous ordering, as well as the porosity of the system, can be tuned over a wide range.

### Conclusion

In conclusion, the amount of poly(ethylene-co-butylene)-b-(ethylene oxide) (PE/B-b-PEO), cetyltrimethylammonium

bromide (CTAB), and the ultrasonication time play important roles in the stability of the miniemulsions and for mesostructure formation. The optimized reaction conditions are a compromise between both stabilization and structuring of the final material. With increasing temperature during ultrasonication, leading to an increased reaction rate, the X-ray diffraction pattern shows a more-pronounced reflection, which indicates a higher degree of ordering. Although a long ultrasonication time inhibits cooperative self-assembly, a high reaction rate at the beginning synthesis step is apparently important to induce mesostructural ordering. We could observe the transformation of porous particles to capsules and finally to flakes with increasing reaction time, which is strongly influenced by the amount of PE/B-b-PEO. With increasing concentration of PE/B-b-PEO, this transformation can be retarded and the porosity as well as the pore size is increased (13 nm instead of 4 nm), indicating that PE/B-b-PEO acts as a structure-directing agent. By simply varying the amount of PE/B-b-PEO or the pH value of the dispersed phase, the morphology and mesostructure formation, as well as the porosity, can be deliberately tuned over a wide range.

**Acknowledgment.** Financial support by Deutsche Forschungsgemeinschaft within the Priority Programm (SPP 1181) is gratefully acknowledged. The authors also thank the Institute of Inorganic Chemistry I (Ulm University) for the synthesis of the precursor, Prof. Dr. Paul Walther for HR-SEM analysis, Conny Egger for BET analysis, Dr. Carola Hoffmann-Richter for AFM analysis, and Samuel Blessing for X-ray measurements.

- 
- (45) Zhao, D.; Feng, J.; Huo, Q.; Melosh, N.; Fredrickson, G. H.; Chmelka, B. F.; Stucky, G. D. Triblock Copolymer Syntheses of Mesoporous Silica with Periodic 50 to 300 Angstrom Pores. *Science* **1998**, 279(5350), 548–552.
  - (46) Khanal, A.; Inoue, Y.; Yada, M.; Nakashima, K. Synthesis of Silica Hollow Nanoparticles Templated by Polymeric Micelle with Core–Shell–Corona Structure. *J. Am. Chem. Soc.* **2007**, 129(6), 1534–1535.